© 2016. Published by The Company of Biologists Ltd | Journal of Cell Science (2016) 129, 2052-2063 doi:10.1242/jcs.183764

RESEARCH ARTICLE

Mapping growth-factor-modulated Akt signaling dynamics

Sean M. Gross[1] and Peter Rotwein[1,2,*]

ABSTRACT

Growth factors alter cellular behavior through shared signaling cascades, raising the question of how specificity is achieved. Here, we have determined how growth factor actions are encoded into Akt signaling dynamics by real-time tracking of a fluorescent sensor. In individual cells, Akt activity was encoded in an analog pattern, with similar latencies (~2 min) and half-maximal peak response times (range of 5–8 min). Yet, different growth factors promoted dose-dependent and heterogeneous changes in signaling dynamics. Insulin treatment caused sustained Akt activity, whereas EGF or PDGF-AA promoted transient signaling; PDGF-BB produced sustained responses at higher concentrations, but short-term effects at low doses, actions that were independent of the PDGF-α receptor. Transient responses to EGF were caused by negative feedback at the receptor level, as a second treatment yielded minimal responses, whereas parallel exposure to IGF-I caused full Akt activation. Small-molecule inhibitors reduced PDGF-BB signaling to transient responses, but only decreased the magnitude of IGF-I actions. Our observations reveal distinctions among growth factors that use shared components, and allow us to capture the consequences of receptor-specific regulatory mechanisms on Akt signaling.

KEY WORDS: Peptide growth factors, Signaling pathways, Signaling dynamics, Akt, Live-cell imaging

INTRODUCTION

Cells interpret their local environment by encoding extracellular cues into intracellular signaling responses. Peptide growth factors are one class of extracellular molecules that stimulate signaling pathways to control cell growth, proliferation or metabolism (Cross and Dexter, 1991). Each of these peptides typically binds to and activates a distinct subset of transmembrane receptors, thereby regulating a variety of intracellular signaling cascades (Lemmon and Schlessinger, 2010). The biochemical steps downstream of each receptor are shared among several classes of growth factors and have been relatively well defined (Lemmon and Schlessinger, 2010; Manning and Cantley, 2007). Yet, different growth factors induce distinctive behavioral responses in cells (Downward, 2001; Marshall, 1995), suggesting that variability in signaling dynamics or other related processes might be key determinants in producing unique biological outcomes.

Previous analyses of signaling dynamics downstream of growth factor receptors have led to several different observations and initial conclusions. For example, PDGF-BB (comprising a heterodimer of two subunits encoded by *PDGFB*) has been found to promote graded short-term activation of the PI3K–Akt pathway (Park et al., 2003), with signaling diminishing over extended time periods (Cirit and Haugh, 2012). By contrast, insulin has been shown to lead to transient or sustained Akt signaling responses (Kubota et al., 2012), as has EGF (Borisov et al., 2009; Chen et al., 2009). In general, as these results have been based on endpoint assays that measure mean responses of a population, the data might not accurately reflect behavior at the single cell level. Additionally, many of these studies did not evaluate the actions of different growth factors in the same cellular context, thus leaving analyses incomplete.

Recently, fluorescent reporter molecules have been developed to track signaling pathways in real time (Nelson et al., 2004; Purvis et al., 2012; Regot et al., 2014; Yissachar et al., 2013). Results generated by using these approaches, have shown not only that signaling dynamics of individual cells tend to be hidden within population averages but also that some pathways yield sustained responses, others produce transient effects and still others show variable patterns depending upon either the strength or duration of the signaling input (Albeck et al., 2013; Batchelor et al., 2011; Nelson et al., 2004; Purvis et al., 2012; Yissachar et al., 2013). Some signaling pathways also have been found to exhibit all-or-none (=digital) outcomes (Tay et al., 2010), whereas others demonstrate graded (=analog) responses (Toettcher et al., 2013). It thus has become apparent that population averages and endpoint assays provide, at best, a limited understanding of overall cellular signaling behavior.

Recently, we have developed a fluorescent reporter protein based on the FoxO1 transcription factor that rapidly and robustly transited from the nucleus to the cytoplasm in response to stimulation of Akt kinase activity (Gross and Rotwein, 2015). With this sensor, we were able to quantify the dynamics of Akt activity over short and longer time courses, and to discover that IGF-I-mediated Akt signaling is encoded into stable and reproducible analog responses at the population level, but that Akt signaling outputs are highly variable among individual cells, particularly after exposure to low growth factor concentrations (Gross and Rotwein, 2015). In this report, we have evaluated Akt signaling dynamics in response to treatment of cells with four different growth factors. Our results provide a quantitative experimental platform for determining how growth factors regulate cellular behavior and reveal the complex nature of how signaling pathways are encoded into different cellular outcomes.

RESULTS

Growth factors and Akt activity

We have previously described a fluorescent reporter protein that was designed to assess Akt activity at the single-cell level (Gross and Rotwein, 2015). The reporter comprises a fusion of the green fluorescent protein Clover (Lam et al., 2012) to the C-terminus of FoxO1, a well-characterized Akt substrate (Brunet et al., 1999; Rena et al., 1999, 2002; Zhang et al., 2002). We modified the FoxO1 portion of the chimeric molecule to inhibit its DNA-binding activity (Tang et al., 1999) and to prevent the effects of phosphorylation by

[1]Department of Biochemistry and Molecular Biology, Oregon Health & Science University, Portland, OR 97239, USA. [2]Department of Biomedical Sciences, Paul L. Foster School of Medicine, Texas Tech Health University Health Sciences Center, El Paso, TX 79905, USA.

*Author for correspondence (peter.rotwein@ttuhsc.edu)

Received 19 November 2015; Accepted 31 March 2016

Journal of Cell Science (2016) 129, 2052-2063 doi:10.1242/jcs.183764

the Mst1 protein kinase (Lehtinen et al., 2006). After lentiviral delivery into cells, stable selection and cell sorting, we were able to visualize rapid and robust reporter transit from the nucleus to the cytoplasm in response to exposure to serum or to the growth factor IGF-I (Gross and Rotwein, 2015).

In order to test how other growth factors regulate Akt signaling activity, we treated the same C3H10T1/2 cells with varying concentrations of insulin, EGF, PDGF-AA (comprising a homodimer of two subunits encoded by *PDGFA*) or PDGF-BB, and monitored real-time responses by live-cell imaging. Each of the growth factors tested engaged a ligand-stimulated tyrosine kinase receptor (Fig. 1A) and activated the PI3K–Akt signaling pathway (Fig. 1B), but through different intermediary molecules (Lemmon and Schlessinger, 2010). Published RNA-seq data from C3H10T1/2 cells shows that mRNAs encoding receptors for each growth factor are expressed, but at different steady-state levels (Fig. 1C) (ENCODE Project Consortium, 2012).

Cells respond in a graded and sustained manner to insulin

The hormone insulin binds both to the insulin receptor and to the IGF-I receptor, although with ∼1000-fold less affinity for the latter (Blakesley et al., 1996). As found previously, the FoxO1–Clover reporter protein was predominantly nuclear in cells incubated in serum-free medium (SFM) (Gross and Rotwein, 2015) (Fig. 1D,F–H). Addition of insulin caused a rapid, dose-dependent and sustained decrease in nuclear levels of FoxO1–Clover, with half-maximal accumulation in the cytoplasm being seen 8–15 min after onset of incubation, and maximal values being attained at ∼20 min (Fig. 1D; Movie 1).

To ascertain whether the reporter was tracking Akt activity, we made serial measurements of both Akt phosphorylation and the phosphorylation of another Akt substrate, PRAS40, by immunoblotting whole-cell protein lysates from cells that had been treated with the highest dose of insulin (1400 pM). Phosphorylation of each Akt and PRAS40 was rapid and sustained, being detected within 5 min of insulin exposure and being maintained over the entire 90-min observation period (Fig. 1E). These results are similar to those observed using the FoxO1–Clover reporter and live-cell imaging (Fig. 1D,H; Movie 1).

The timecourse studies and immunoblotting results in Fig. 1C,D represent population averages, and do not provide insight into the behavior of individual cells exposed to different hormone concentrations. We therefore examined the single-cell data from which the population averages were derived and found that responses to insulin were variable, particularly at lower hormone concentrations (170 pM) (Fig. 1F; Fig. S1D). Upon exposure to higher concentrations of insulin (1400 pM), initial rates and the extent of export of the FoxO1–Clover reporter from the nucleus were more substantial and less heterogeneous than those at lower hormone concentrations (Fig. 1G; Fig. S1D). Taken together, the results in Fig. 1 show that, like those in response to IGF-I (Gross and Rotwein, 2015), the effects of a given concentration of insulin on individual cells are graded, with exposure to higher hormone levels leading to more sustained and less variable outcomes than lower concentrations.

Cells respond transiently to EGF

To test whether graded and sustained responses are the standard pattern for how growth factor signals are encoded into Akt activity, we next exposed cells to different concentrations of EGF. EGF-mediated signaling is complicated because the growth factor can bind to any of three receptors – EGFR (ErbB1), ErbB3 or ErbB4 – but with different affinities (Citri and Yarden, 2006; Riese et al., 2007), leading to a variety of homo- and hetero-dimers, including those containing ErbB2, which on its own lacks growth-factor-binding capabilities (Citri and Yarden, 2006; Riese et al., 2007). Addition of EGF to cells that had been pre-incubated in SFM caused rapid, dose-dependent and transient decreases in nuclear levels of the FoxO1–Clover reporter protein. At the population level, half-maximal accumulation of the reporter in the cytoplasm was observed 6–9 min after EGF treatment, with maximal values being reached by ∼13 min and signal intensity waning by 45 min (Fig. 2A; Movie 2). Similarly, transient effects were seen by immunoblotting treated cells for phosphorylation of Akt or of PRAS40 (Fig. 2B). Transient effects were also observed at the single-cell level, where growth-factor-mediated signaling was found to be highly heterogeneous at both lower and higher concentrations of EGF (Fig. 2C–F; Fig. S1B). As noted in Fig. 2F, the timing of the responses of individual cells to EGF in terms of nuclear-to-cytoplasmic translocation of the FoxO1–Clover reporter molecule was fairly similar, even when stratified by overall EGF activity, although a larger fraction of cells reached a peak earlier compared to that of cells exhibiting a lower maximal response.

We next asked if these transient signaling responses to EGF are caused by a negative-feedback loop. Such processes could inhibit Akt signaling at the level of EGF receptors or act further downstream, thus, preventing another growth factor from activating Akt. To address this question, cells were first incubated with EGF (4.2 nM) for 60 min, followed by the addition of EGF (4.2 nM) or IGF-I (500 pM). We found that a second treatment with EGF minimally promoted FoxO1–Clover reporter translocation out of the nucleus (Fig. 2G). In contrast, addition of IGF-I caused a rapid, extensive and sustained signaling response (Fig. 2G). These results show that negative feedback of EGF-mediated signaling in C3H10T1/2 cells is located upstream of the PI3K–Akt module and is likely to occur at the level of the receptor.

Variable responses of the FoxO1–Clover reporter protein to PDGF-AA or PDGF-BB

We next exposed cells to different concentrations of PDGF-AA or PDGF-BB. These two growth factors function as dimers and vary in their affinity for PDGF-α and PDGF-β receptors (Andrae et al., 2008). PDGF-AA binds almost exclusively to the PDGF-α receptor, whereas PDGF-BB binds to both receptors (Andrae et al., 2008) (Fig. 1A). Cells that had been incubated with PDGF-AA showed rapid, dose-dependent decreases in nuclear levels of FoxO1–Clover, with half-maximal accumulation in the cytoplasm by 6–10 min and maximal values by ∼14 min (Fig. 3A; Movie 3). In contrast to the effects of insulin, but similar to EGF, population responses to PDGF-AA were transient because they declined by 50–75% from peak values over the next 40 min (Fig. 3A). Similarly, brief effects were seen for PDGF-AA-stimulated phosphorylation of Akt and PRAS40, as measured by immunoblotting of cells that had been incubated with the highest concentration of growth factor (1400 pM) (Fig. 3B).

Analysis of single-cell data that had been obtained by live-cell imaging revealed that individual responses to PDGF-AA were highly variable. At both lower (140 pM) and higher concentrations of growth factor (1400 pM), the effects of PDGF-AA ranged from minimal and transient to substantial and sustained (Fig. 3C–E). These results illustrate that population averages serve as a poor proxy for signaling responses to PDGF-AA at the single-cell level.

To further quantify the effects of PDGF-AA on individual cells, we clustered all of the single-cell responses into four distinct groups

Journal of Cell Science (2016) 129, 2052-2063 doi:10.1242/jcs.183764

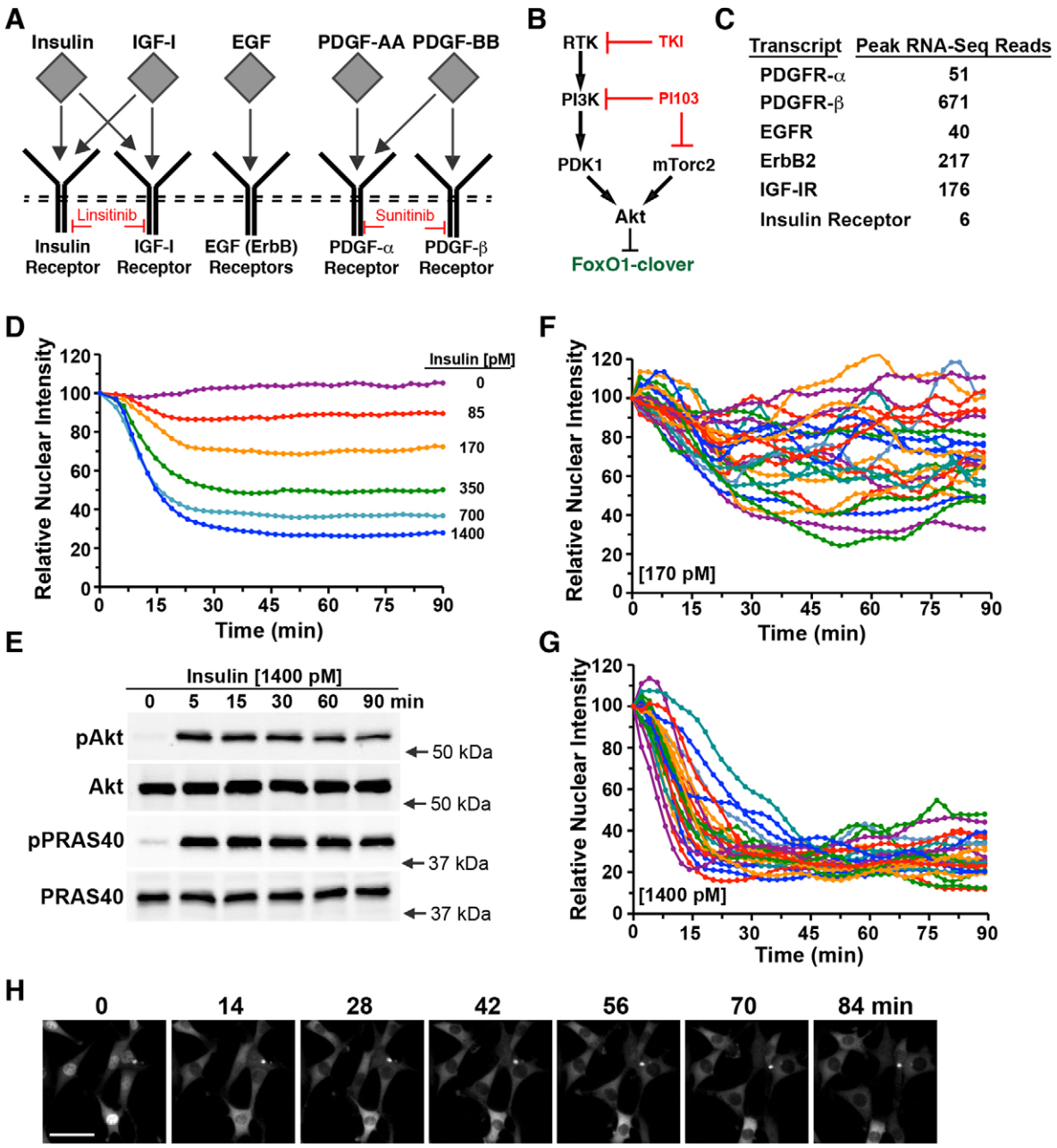

Fig. 1. Graded responses of the FoxO1–Clover reporter to different concentrations of insulin. (A) Overview of growth factor signaling studied in this article. Binding of insulin, IGF-I, EGF, PDGF-AA and PDGF-BB to their respective tyrosine kinase receptors. The locations of action of the small-molecule tyrosine kinase inhibitors Linisitib and Sunitinib are indicated. (B) Diagram of steps leading to activation of Akt and its regulation of the FoxO1–Clover reporter protein. The targets of various inhibitors are depicted. RTK, receptor tyrosine kinase; TKI, tyrosine kinase inhibitor; PI103, small-molecule inhibitor of PI3-kinase (PI3K) and mTorc2. (C) The relative amount of each receptor mRNA is listed, calculated using previously published RNA seq data, as described in Materials and Methods. (D) Time course of relative nuclear intensity of the FoxO1–Clover reporter in C3H10T1/2 cells first incubated in SFM, and following exposure to different concentrations of insulin for 90 min. Population means are presented (n=100 cells per incubation from two independent experiments). The nuclear intensity of the reporter in each cell was normalized to its value at the start of imaging during incubation in SFM. (E) Expression of phosphorylated Akt at residue T308 (pAkt), total Akt, phosphorylated PRAS40 at residue T246 (pPRAS40) and total PRAS40 by immunoblotting using whole-cell protein lysates from cells exposed to insulin (1400 pM) for up to 90 min. Molecular mass markers are indicated to the right of each immunoblot. (F,G) Timecourse results for each of 25 cells incubated with insulin for 90 min (F, 170 pM; G, 1400 pM). (H) Time-lapse images from a representative experiment showing changes in the subcellular location of the FoxO1–Clover reporter in cells that had been exposed to insulin (1400 pM) for the times indicated. Scale bar: 50 µM.

based on signaling dynamics, using relative nuclear intensity of the FoxO1–Clover reporter at 18- and 90-min time points as a guide. We grouped the results as showing no response, a small transient effect, a larger transient response, or large and sustained effects (Fig. 4A,B; Fig. S1A). When these results were graphed based on PDGF-AA concentrations, it could be seen that as the growth factor dose rose, the fraction of cells demonstrating more extensive responses increased (Fig. 4C). However, even at the two highest concentrations of PDGF-AA, 25–30% of cells showed no or minimal responses and only 10–15% demonstrated sustained effects (Fig. 4C).

The signaling dynamics of cells that had been treated with PDGF-BB were different from those incubated with PDGF-AA. At lower

Journal of Cell Science (2016) 129, 2052-2063 doi:10.1242/jcs.183764

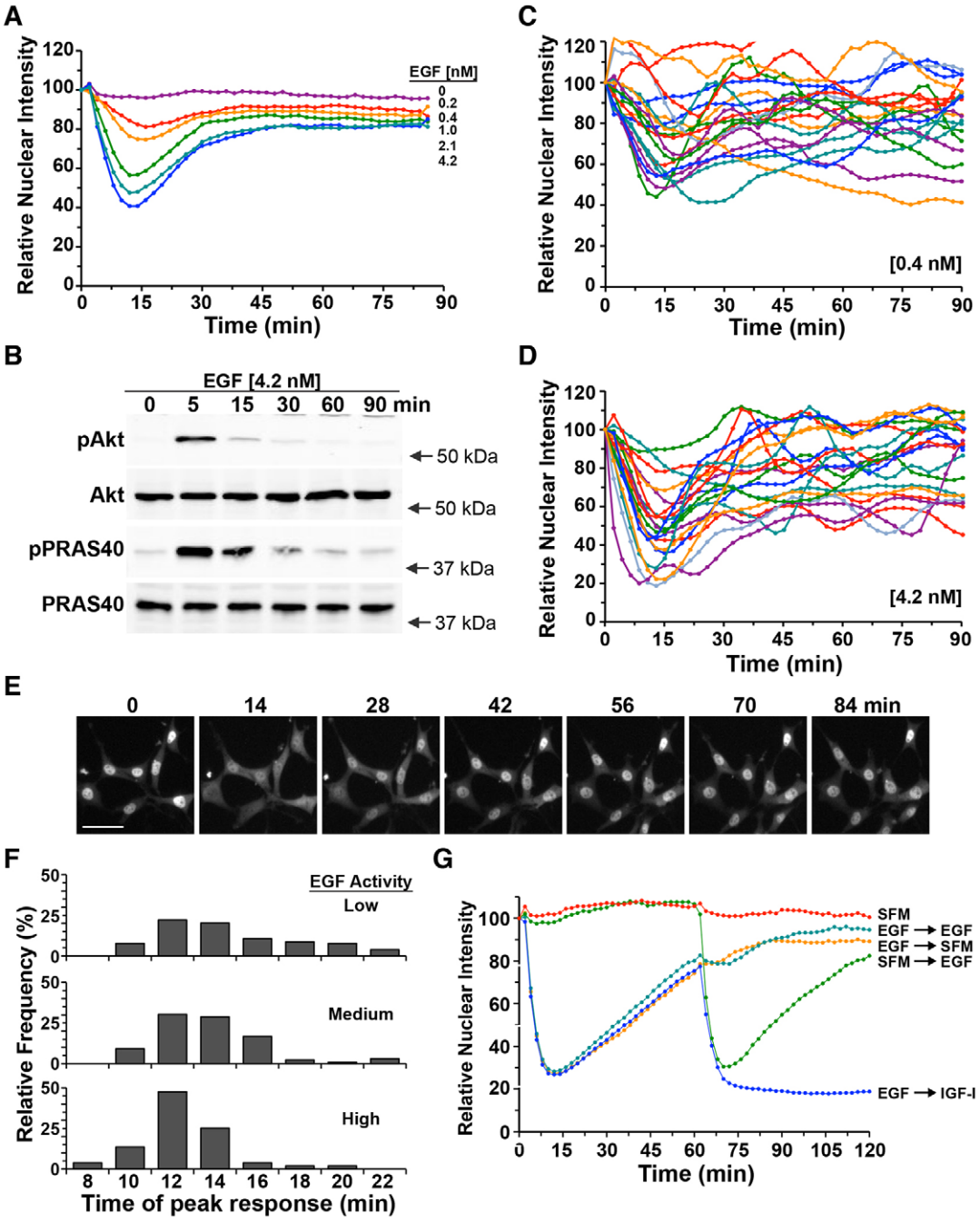

Fig. 2. Responses of the FoxO1–Clover reporter to different concentrations of EGF. (A) Time course of relative nuclear intensity of the FoxO1–Clover reporter in C3H10T1/2 cells incubated first in SFM, and following exposure to different concentrations of EGF for 90 min. Population means are presented (*n*=100 cells per incubation from two independent experiments). The nuclear intensity of the reporter in each cell was normalized to its value at the start of imaging during incubation in SFM. (B) Expression of phosphorylated Akt (pAkt), total Akt, phosphorylated PRAS40 (pPRAS40) and total PRAS40 by immunoblotting using whole-cell protein lysates from cells exposed to EGF (4.2 nM) for up to 90 min. Molecular mass markers are illustrated to the right of each immunoblot. (C,D) Timecourse results for each of 25 cells incubated with EGF for 90 min (C, 0.4 nM; D, 4.2 nM). (E) Time-lapse images from a representative experiment showing changes in the subcellular location of the FoxO1–Clover reporter in cells exposed to EGF (4.2 nM) for the times indicated. Scale bar: 50 µM. (F) Histograms for individual cells exposed to different concentrations of EGF showing the frequency of the time to peak response (~100 cells per group). The terms 'Low', 'Medium' and 'High' refer to the level of peak EGF-mediated signaling activity. (G) Repeated exposure to EGF yields reduced population responses. Time course of relative nuclear intensity of the FoxO1–Clover reporter in C3H10T1/2 cells incubated with SFM (red tracing), with EGF (4.2 nM; orange), sequentially with two exposures to EGF (aqua), with SFM followed by EGF (green) or with EGF followed by IGF-I (500 pM, blue). Population averages are presented (*n*=50 cells per incubation).

growth factor concentrations, the mean response of the FoxO1–Clover reporter was transient and resembled effects of PDGF-AA, with half-maximal accumulation in the cytoplasm by 8–9 min, and maximal values by ~14 min (Fig. 5A; Movie 4). In contrast, at higher concentrations of PDGF-BB, signaling responses were more rapid and extensive because half-maximal accumulation of FoxO1–Clover in the cytoplasm was seen at ~5 min and cytoplasmic localization of the reporter was maintained for at least 90 min

Journal of Cell Science (2016) 129, 2052-2063 doi:10.1242/jcs.183764

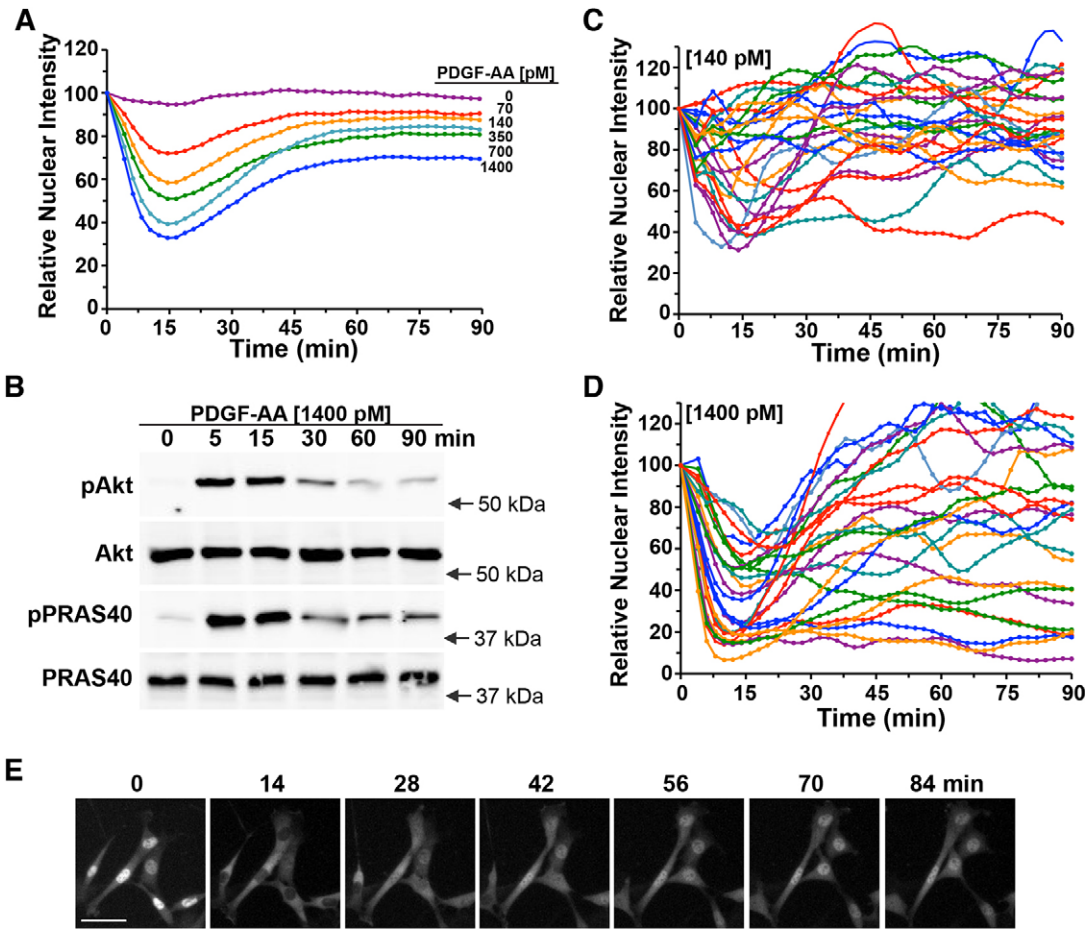

Fig. 3. Responses of the FoxO1–Clover reporter to different concentrations of PDGF-AA. (A) Time course of relative nuclear intensity of the FoxO1–Clover reporter in C3H10T1/2 cells incubated in SFM followed by exposure to different concentrations of PDGF-AA for 90 min. Population means are presented (*n*=150 cells per incubation from three independent experiments). The nuclear intensity of the reporter in each cell was normalized to its value at the start of imaging during incubation in SFM. (B) Expression of phosphorylated Akt (pAkt), total Akt, phosphorylated PRAS40 (pPRAS40) and total PRAS40 by immunoblotting using whole-cell protein lysates from cells exposed to PDGF-AA (1400 pM) for up to 90 min. Molecular mass markers are illustrated to the right of each immunoblot. (C,D) Timecourse results for each of 25 cells incubated with PDGF-AA for 90 min (C, 140 pM; D, 1400 pM). (E) Time-lapse images from a representative experiment showing changes in the subcellular location of the FoxO1–Clover reporter in cells exposed to PDGF-AA (1400 pM) for the times indicated. Scale bar: 50 µM.

(Fig. 5A). Similarly, sustained signaling was seen in immunoblots of Akt and PRAS40 phosphorylation after exposure of cells to the highest concentrations of PDGF-BB (104 pM) (Fig. 5B).

Analysis of individual cells confirmed the dose-dependent heterogeneity of signaling responses to PDGF-BB. At low concentrations of growth factor (5.2 pM), effects on individual cells were highly variable, with some cells showing no changes in the nuclear localization of the FoxO1–Clover reporter and others maintaining sustained cytoplasmic translocation (Fig. 5C). In contrast, upon exposure to the highest concentrations of growth factor (104 pM), the effects of PDGF-BB were similar to those seen with the highest concentrations of insulin because the reporter was rapidly translocated to the cytoplasm in nearly all cells and was maintained there for the 90-min duration of the experiment (Fig. 5D,E). When individual cellular responses to PDGF-BB were graphed using the same criteria as those used for PDGF-AA, the results also showed dose-dependent effects ranging from small and transient to large and sustained signaling, but with sharper and more complete transitions than were observed for PDGF-AA – at peak concentrations of PDGF-BB, 90–99% of cells showed large and sustained signaling responses (Fig. 5F,G; Fig. S1C).

The signaling dynamics initiated by PDGF-BB reflect combined engagement of both PDGF-α and PDGF-β receptors, whereas the effects of PDGF-AA are mediated solely by PDGF-α receptors (Andrae et al., 2008). To identify the signaling that occurs exclusively through PDGF-β receptors, we incubated cells with a neutralizing antibody to PDGF-α. In the presence of antibody, signaling by PDGF-AA was completely inhibited, whereas exposure of cells to control IgG had no effect (Fig. 6A). In contrast, the same antibody against PDGF-α reduced responses to submaximal concentrations of PDGF-BB by only ∼10%, had no effect at the highest PDGF-BB dose (Fig. 6B) and did not alter single-cell dynamics (Fig. 6C). Taken together, the results in Figs 4–6 demonstrate remarkable plasticity in PDGF-mediated signaling dynamics for Akt that appear to be dependent on the type and amount of PDGF receptor being activated.

Chemical inhibitors recapitulate dose-dependent PDGF-BB signaling

As seen in Figs 5 and 6, signaling by PDGF-BB became stronger and more sustained as cells were exposed to higher growth factor concentrations. To understand the mechanisms behind this process

Journal of Cell Science (2016) 129, 2052-2063 doi:10.1242/jcs.183764

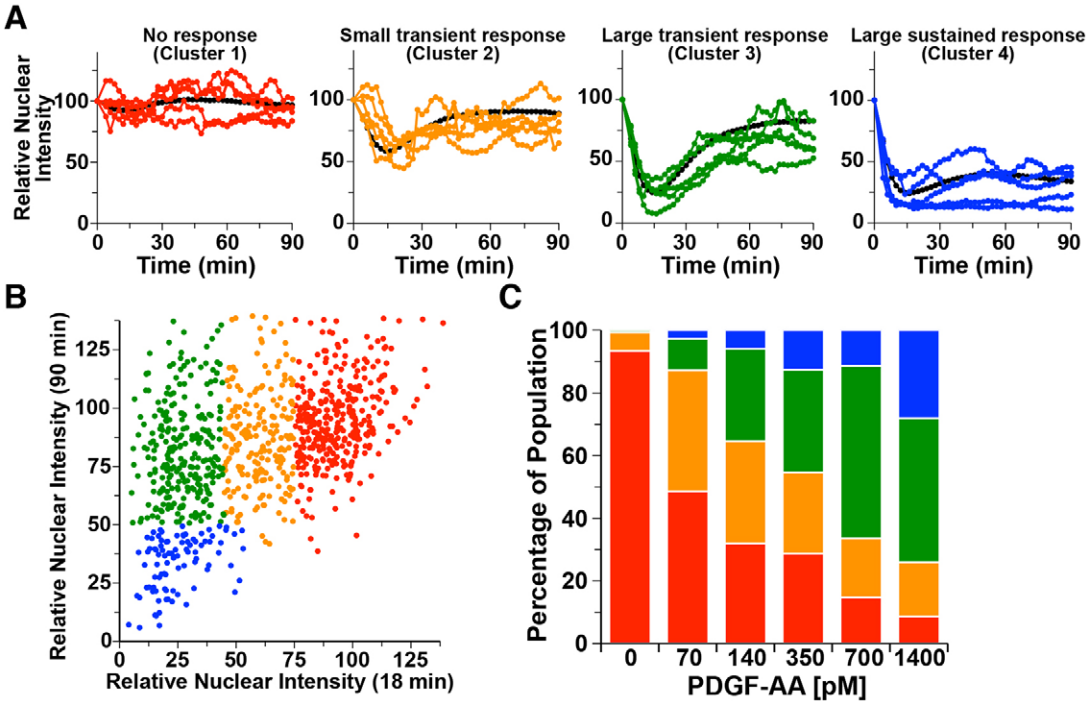

Fig. 4. Defining PDGF-AA-mediated signaling patterns. (A) Presentation of representative single-cell traces based on the type of response seen after incubation with PDGF-AA: no response is illustrated by the graph with the red lines; small transient responses are shown in gold; stronger transient responses are in green, and strong sustained responses are in blue. The black line in each graph shows the average response across that cluster. (B) Dot-plot illustrating the correlation of responses of individual cells after incubation with PDGF-AA at 18 and 90 min after growth factor addition (n=900 cells). Color-coding is identical to that in A. (C) Bar graphs showing the fraction of cells in the population responding to incubation with different concentrations of PDGF-AA. Color-coding is identical to that in A.

and to learn how the downstream Akt signaling pathway is wired, we incubated cells with different amounts of the PDGF receptor tyrosine kinase inhibitor Sunitinib in the presence of high concentrations of PDGF-BB. Under these conditions, Sunitinib caused a dose-dependent shift from sustained to more transient Akt activity, as measured by the subcellular location of the FoxO1–Clover reporter (Fig. 7A). Similar results were observed with the dual PI3K and mTor inhibitor PI103, which more directly blocks Akt signaling (Fig. 7B). Thus, it appears that inhibiting either the receptor or downstream pathway activity recapitulates signaling dynamics from submaximal PDGF-BB stimulation.

To learn more generally if inhibition of different components of a signaling pathway has comparable effects, we exposed cells to graded concentrations of the IGF-I-insulin-receptor-specific tyrosine kinase inhibitor Linsitinib or to PI103. In contrast to results with PDGF-BB, each inhibitor caused a dose-dependent decline in maximal IGF-I-mediated cytoplasmic localization of the FoxO1–Clover reporter molecule, but did not reduce the duration of signaling (Fig. 7C,D). Moreover, PI103 was more effective in blocking PDGF-BB-stimulated Akt activity than in blunting IGF-I actions because the IC_{50} for PDGF-BB-mediated signaling was between 20 and 50 nM, whereas for IGF-I it was between 50 and 200 nM (compare Fig. 7B and D). These results show how inhibitors can reveal variability within a common downstream pathway regulated by different upstream activators.

General variability in growth-factor-signaling dynamics

To more broadly assess the dynamics of signaling by different growth factors and their receptors, we also developed a HeLa cell line that stably expressed the FoxO1–Clover reporter protein. In HeLa FoxO1–Clover-expressing cells, IGF-I (500 pM) and insulin (1400 pM) produced sustained signaling effects, whereas EGF (4.2 nM) and PDGF-BB (4.1 nM) caused transient responses (Fig. 8A). Treatment with PDGF-AA (3.5 nM) was ineffective, as presumably HeLa cells lack specific receptor expression. Analysis by live-cell imaging of individual cells confirmed the different response patterns observed at the population level (Fig. 8B–E). Although there was some variability, IGF-I [and insulin (not shown)] caused sustained effects, whereas responses to both EGF and PDGF-BB were more transient and heterogeneous (Fig. 8B–E). Thus, variation in signaling dynamics among different growth factors, as assessed by live-cell imaging, appears to be a general property that is not unique to a single cell line.

DISCUSSION

Peptide growth factors influence cellular behavior by engaging transmembrane receptors and activating a broad range of intracellular signaling responses (Downward, 2001). Although each growth factor typically binds to a unique receptor, many of the downstream signaling cascades are shared, leading to the question of how different growth factors cause specific behavioral responses. Here, we have examined the effects of several growth factors on the PI3K–Akt signaling pathway by using a recently developed sensor that comprised a fusion between a modified FoxO1 transcription factor and the green fluorescent protein Clover (Gross and Rotwein, 2015). Our results reveal how different growth factors can encode distinct cellular behaviors, and elucidate new information about the dynamics of the PI3K–Akt pathway.

Population dynamics of growth factor signaling

We have shown recently with live-cell imaging that IGF-I promotes long-term activation of PI3K–Akt signaling in cultured fibroblasts

Journal of Cell Science (2016) 129, 2052-2063 doi:10.1242/jcs.183764

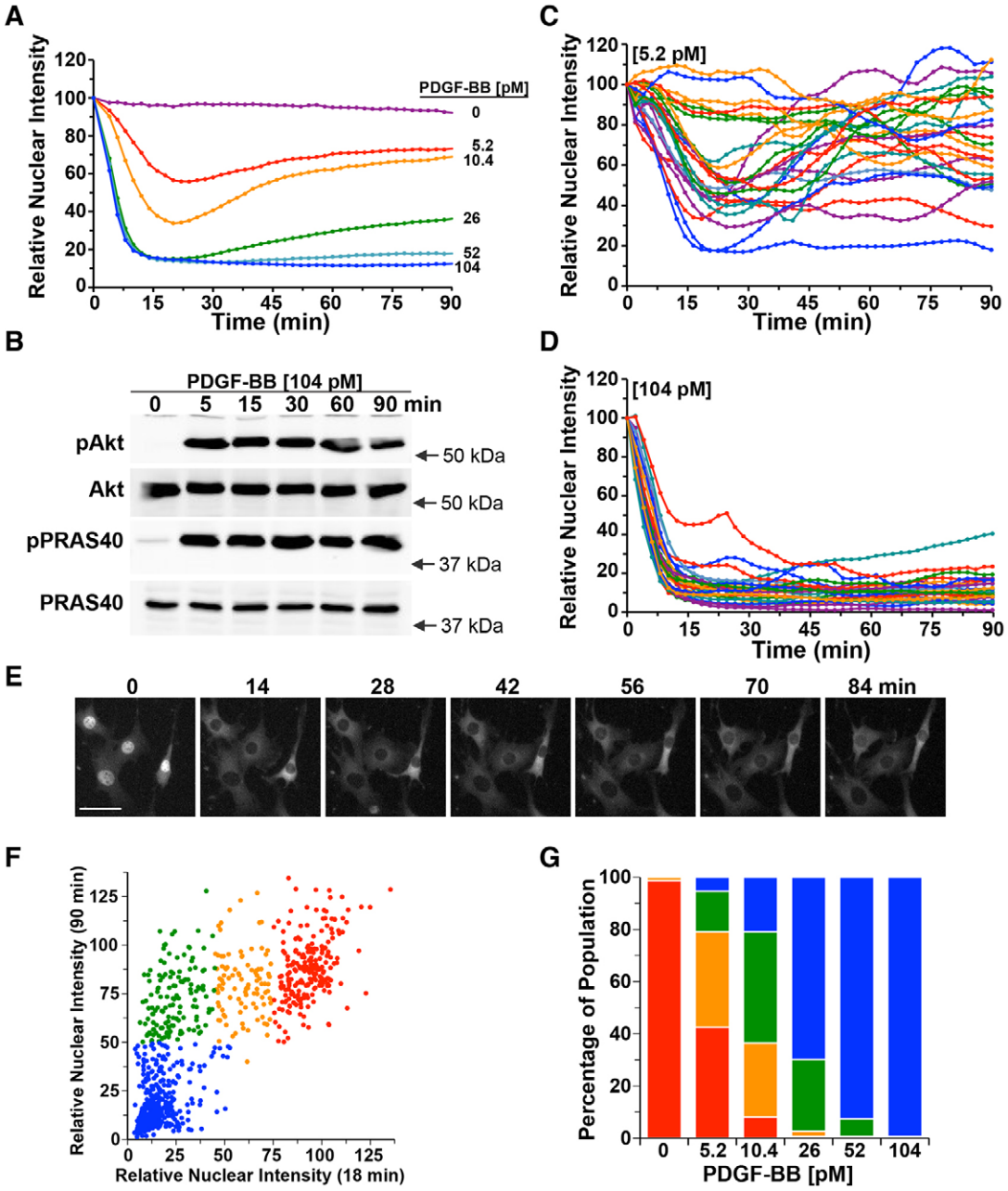

Fig. 5. Graded responses of the FoxO1–Clover reporter to different concentrations of PDGF-BB. (A) Time course of relative nuclear intensity of the FoxO1–Clover reporter in C3H10T1/2 cells first incubated in SFM then followed by exposure to different concentrations of PDGF-BB for 90 min. Population means are depicted (n=150 cells per incubation from three independent experiments). The nuclear intensity of the reporter in each cell was normalized to its value at the start of imaging during incubation in SFM (=100). (B) Expression of phosphorylated Akt (pAkt), total Akt, phosphorylated PRAS40 (pPRAS40) and total PRAS40 by immunoblotting using whole-cell protein lysates from cells exposed to PDGF-BB (104 pM) for up to 90 min. Molecular mass markers are shown to the right of each immunoblot. (C,D) Timecourse results for each of 25 cells incubated with PDGF-BB for 90 min (C, 5.2 pM; D, 104 pM). (E) Time-lapse images from a representative experiment showing changes in the subcellular location of the FoxO1–Clover reporter in cells exposed to PDGF-BB [104 pM] for the times indicated. Scale bar: 50 µM. (F,G) Defining patterns of PDGF-BB-mediated signaling. (F) Dot-plot illustrating the pattern of responses of individual cells after incubation with PDGF-BB at 18 and 90 min after growth factor addition (n=900 cells). Color-coding is identical to that in Fig. 4. (G) Bar graphs showing the fraction of cells in the population responding to incubation with different concentrations of PDGF-BB. Color-coding is identical to that in Fig. 4.

and myoblasts (Gross and Rotwein, 2015). Exposure of cells to IGF-I leads to sustained Akt signaling responses that showed dose-dependent increases in magnitude, as measured by the fraction of the fluorescent FoxO1–Clover reporter protein that had translocated from the nucleus to the cytoplasm. At the population level, more cytoplasmic localization of the reporter correlates with more Akt phosphorylation and with increased phosphorylation of another Akt substrate, as seen by immunoblotting (Gross and Rotwein, 2015). These results prompted us to investigate how other growth factors encode their tyrosine kinase receptors into Akt signaling dynamics.

We now find that different growth factors induce distinct patterns of Akt activity. Like IGF-I, exposure of cells to insulin led to sustained Akt signaling, with concentration-dependent increases in the fraction of the FoxO1–Clover sensor that translocated out of the nucleus (Fig. 1C). By contrast, incubation of cells with EGF promoted more transient signaling, as evidenced by an early dose-

Journal of Cell Science (2016) 129, 2052-2063 doi:10.1242/jcs.183764

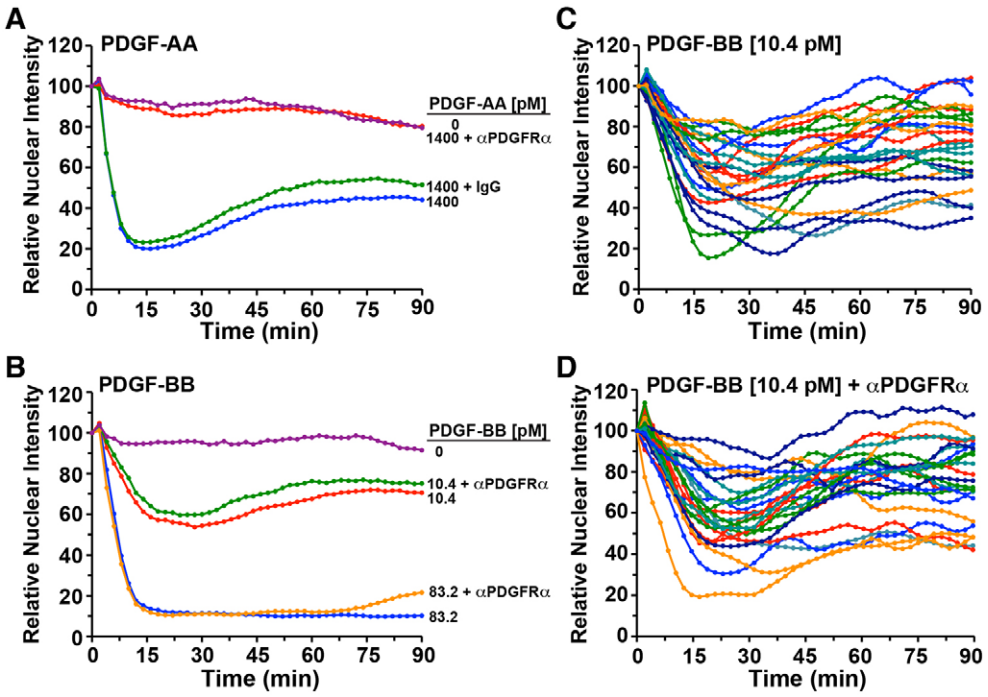

Fig. 6. Preventing PDGF-AA-mediated signaling by blocking the PDGF-α receptor. (A) Time course of relative nuclear intensity of the FoxO1–Clover reporter in C3H10T1/2 cells incubated in SFM and followed by exposure to PDGF-AA (1400 pM) for 90 min with or without either an antibody against PDGF-α receptor (αPDGFRα) or an IgG control. (B) Time course of relative nuclear intensity of the FoxO1–Clover reporter in C3H10T1/2 cells incubated in SFM and followed by exposure to different concentrations of PDGF-BB for 90 min with or without αPDGFRα. In both A and B, population means are presented (*n*=50 cells). The nuclear intensity of the reporter in each cell was normalized to its value at the start of imaging during incubation in SFM (=100). (C,D) Timecourse results for each of 25 cells incubated with PDGF-BB for 90 min (C, 10.4 pM; D, 10.4 pM plus αPDGFRα).

dependent peak of reporter accumulation in the cytoplasm, followed by a gradual decline back toward baseline levels (Fig. 2A). These latter results agree with some previous observations in which Akt is transiently activated by EGF (Borisov et al., 2009), although, in many other studies in multiple cell types, Akt signaling is maintained for long durations after EGF treatment (Chen et al., 2009).

Exposure of cells to PDGF-AA or PDGF-BB led to more complex signaling patterns. At low PDGF-BB concentrations, population responses resembled those seen with the highest levels of PDGF-AA, with an initial rapid peak of cytoplasmic translocation of the Akt reporter followed by a gradual return to the nucleus (Fig. 5A). These results were not caused by rapid degradation of growth factor in the extracellular environment because the same transient response was recapitulated in the presence of high PDGF-BB concentrations upon small-molecule pathway inhibition (Fig. 7A,B). Similarly, there did not appear to be preferential activation of the PDGF-α receptor by PDGF-BB because specific inhibition of the receptor with an antibody had minimal effects on signaling dynamics (Fig. 6). At higher concentrations of PDGF-BB, Akt activity was more sustained (Fig. 5A), with signaling resembling the patterns of insulin or IGF-I (Gross and Rotwein, 2015). Previous studies in 3T3 fibroblasts that have tracked Akt phosphorylation by serial immunoblotting show similar dose-dependent results (Cirit and Haugh, 2012), but they did not note the complicated signaling dynamics that we have observed by live-cell imaging. PDGF signaling responses also differed in HeLa cells because PDGF-AA was ineffective and PDGF-BB produced only transient responses (Fig. 8A), indicating that other factors, such as the total number of receptors, significantly influences PDGF-BB signaling dynamics.

Growth-factor-signaling dynamics in individual cells

For all growth factors tested, responses in individual cells varied dramatically, with some cells showing rapid and maximal redistribution of the FoxO1–Clover reporter protein from the nucleus to the cytoplasm after growth factor exposure, and others responding minimally. For insulin and PDGF-BB [and IGF-I (Gross and Rotwein, 2015)], single cells in the population yielded more consistent and extensive responses after incubation with higher growth factor concentrations (Figs 1 and 5; Fig. S1C,D). This was not true for EGF or PDGF-AA, where signaling was highly heterogeneous regardless of growth factor dose (Figs 2–4; Fig. S1A,B). Collectively, our studies show that population averages provide a poor measure of single cell behavior and illustrate an important advantage of live-cell imaging over the more static measurements of endpoint assays as the former approach makes it possible to capture the full range of cellular signaling activity.

Although our observations demonstrate that Akt signaling dynamics are highly variable among the cells in a population, they also illustrate some fundamental similarities. First, in all of our experiments, Akt activity appears to be encoded in an analog pattern, with different growth factors promoting dose-dependent changes in the peak response, rather than signaling in an all-or-none, or digital, manner. Second, we found that signaling latency was consistent among different growth factors, with the initial subcellular relocation of the FoxO1–Clover reporter being measured within ∼2 min after growth factor addition to cells (see Movies 1–4). Third, the half-maximal peak response to the highest growth factor concentration was recorded at a similar time, within 5–8 min after initial exposure. Thus, tracking signaling activity from multiple growth factors by live-cell imaging in the same cellular background can reveal commonalities of signaling patterns as well as unique differences.

Wiring of receptor–Akt interactions

Exposure of cells to IGF-I produced sustained activation of Akt, but EGF induced only transient signaling (Fig. 2A–E; Gross and Rotwein, 2015). Sequential incubation of cells with EGF yielded a minimal second response, but prior exposure to EGF did not block full Akt activation by IGF-I (Fig. 2G). Thus, negative feedback for EGF-mediated signaling probably resides at the level of EGF receptors and not within the downstream PI3K–Akt module.

Journal of Cell Science (2016) 129, 2052-2063 doi:10.1242/jcs.183764

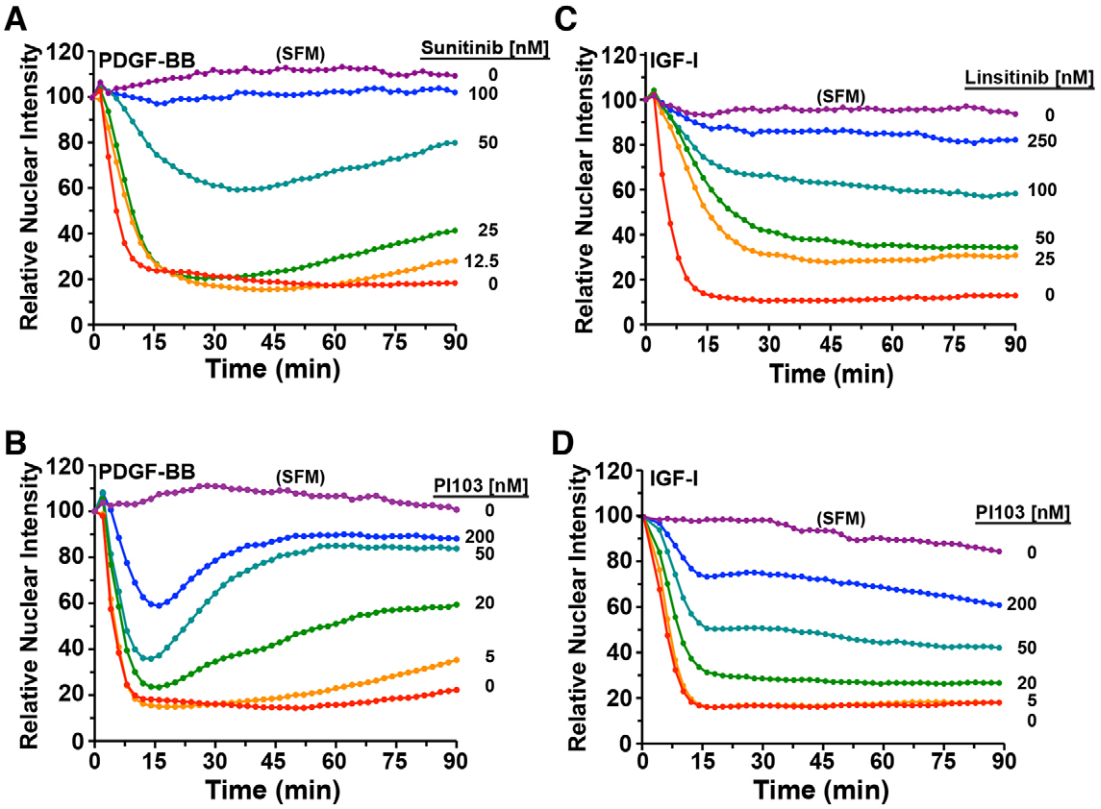

Fig. 7. Dose-dependent effects of small-molecule inhibitors on growth-factor-mediated signaling. (A) Time course of relative nuclear intensity of the FoxO1–Clover reporter in C3H10T1/2 cells incubated with SFM or PDGF-BB (830 pM) for 90 min in the presence of various concentrations of the receptor tyrosine kinase inhibitor Sunitinib. Population averages are presented (*n*=50 cells per incubation). (B) Time course of relative nuclear intensity of the FoxO1–Clover reporter in cells incubated with SFM or PDGF-BB (830 pM) for 90 min in the presence of different concentrations of PI103. Population averages are presented (*n*=50 cells per incubation). (C) Time course of relative nuclear intensity of the FoxO1–Clover reporter in cells incubated with SFM or IGF-I (500 pM) for 90 min in the presence of various concentrations of the receptor tyrosine kinase inhibitor Linsitinib. Population averages are presented (*n*=50 cells per incubation). (D) Time course of relative nuclear intensity of the FoxO1–Clover reporter in cells incubated with SFM or IGF-I (500 pM) for 90 min in the presence of different concentrations of PI103. Population averages are presented (*n*=50 cells per incubation).

Negative feedback is thus likely to be secondary to receptor internalization kinetics or dynamics (Goh and Sorkin, 2013), the presence of an inducible receptor inhibitor – such as Mig6 (Anastasi et al., 2016) – or other receptor-associated modulatory proteins (Kaushansky et al., 2008). This pattern of limited responsiveness to sequential growth factor treatment observed with EGF also differs from what we found previously with IGF-I, in which a second exposure to growth factor promoted a strong signaling response that was nearly identical to that upon the initial treatment (Gross and Rotwein, 2015). This comparison reveals that, depending on the growth factor and receptor, previous signaling history can have either a large or insignificant impact on subsequent activity.

The application of inhibitors that perturbed different signaling components allowed us also to identify potential wiring principles that govern the relationship between the PI3K–Akt module and different receptor tyrosine kinases. Blockade of both PDGF receptors with the small molecule Sunitinib reduced sustained maximum responses to a dose-dependent transient effect (Fig. 7A), as did inhibition of Akt activation with PI103, thus recapitulating the pattern seen with PDGF-AA or with low concentrations of PDGF-BB (compare Fig. 7B with Fig. 5A). Different results were observed when IGF-I-mediated Akt activity was blocked. Addition of PI103 or the IGF-I receptor kinase inhibitor Linsitinib each reduced the magnitude but not the duration of FoxO1–Clover reporter translocation in response to IGF-I. Collectively, these observations suggest that regulation of signaling dynamics primarily occurs at the receptor level and not further downstream, where shared components are used.

Advantages of live-cell imaging in understanding signaling pathways

Variable conclusions about population responses to different growth factors have been reached by more traditional endpoint assays, including the use of serial immunoblotting or immunocytochemistry to probe for Akt or substrate phosphorylation (Borisov et al., 2009; Chen et al., 2009; Kubota et al., 2012; Park et al., 2003). Here, by continuous monitoring, we were able to collect a consistent and more robust data set with less experimental effort and fewer assumptions. Furthermore, we were able to observe aspects of Akt signaling in individual cells that is not possible with other experimental approaches. For example, using immunoblots it is difficult to distinguish between analog and digital responses, or to detect differences in peak signaling activity and timing because of the limited temporal and dynamic resolution of this modality. Although immunocytochemical studies can give insights into signaling in individual cells, they require the assumption that different cells are equivalent and that all cells respond synchronously, which we find is not true. Furthermore, repeated stimuli cannot be tracked using this approach without an inordinately large number of controls, and studies such as those addressing combinatorial growth factor signaling or the effects of different inhibitors on signaling dynamics and

Journal of Cell Science (2016) 129, 2052-2063 doi:10.1242/jcs.183764

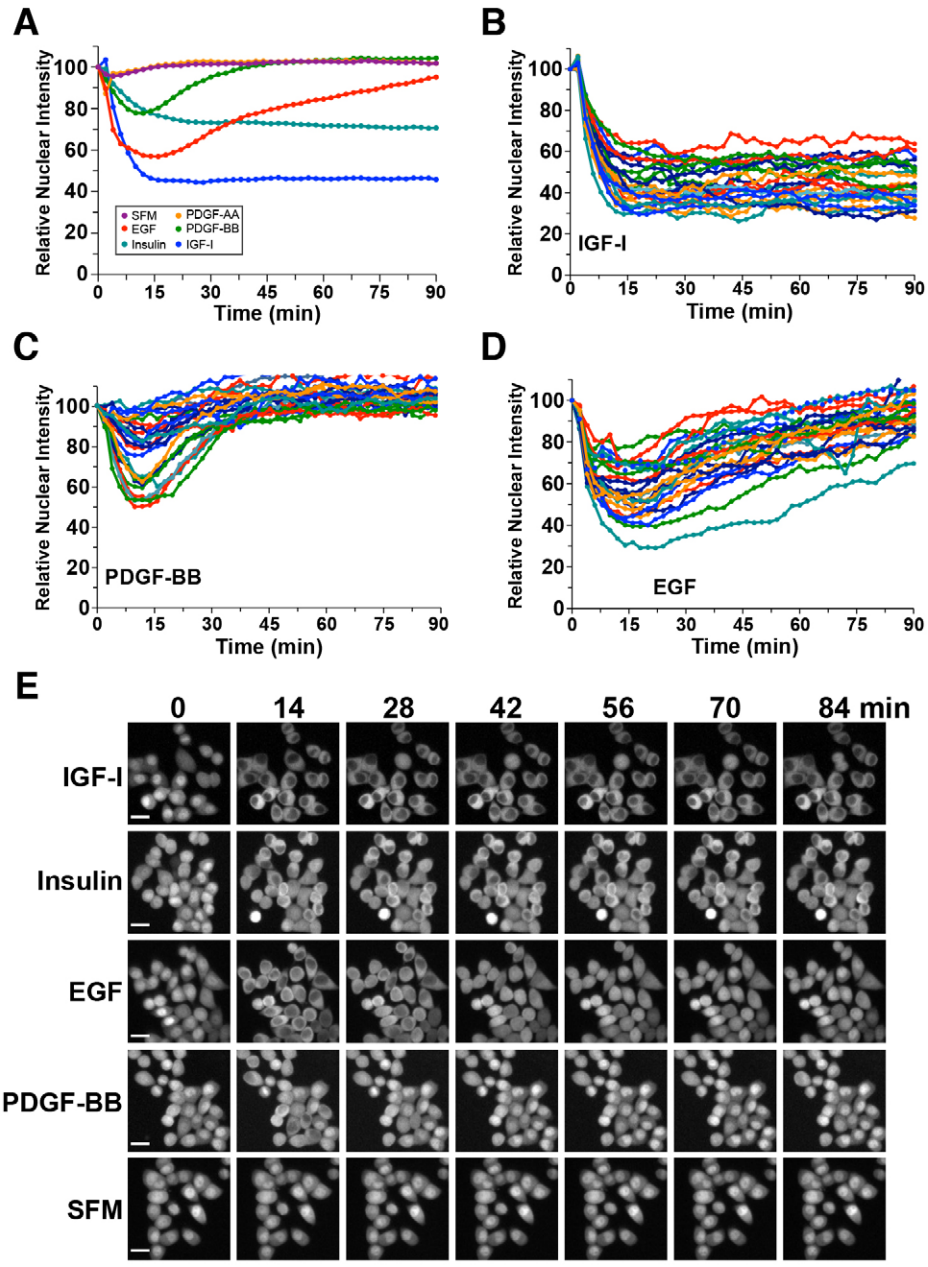

Fig. 8. Distinct growth factor actions in HeLa cells. (A) Time course of the relative nuclear intensity of the FoxO1–Clover reporter in HeLa cells first incubated in SFM and then exposed to different growth factors for 90 min. Population means are depicted (*n*=50 cells per incubation). The nuclear intensity of the reporter in each cell was normalized to its value at the start of imaging during incubation in SFM (=100). (B–E) Time course results for each of 25 cells incubated with IGF-I (B, 500 pM), PDGF-BB (C, 4.1 nM) or EGF (D, 4.2 nM). (E) Time-lapse images from a representative experiment showing changes in the subcellular location of the FoxO1–Clover reporter in cells exposed to different growth factors for the times indicated. Scale bars: 25 µM.

kinetics cannot be performed accurately. Thus, experiments using real-time live-cell imaging and a fluorescent reporter can reveal a wealth of signaling information that is not otherwise attainable.

Implications of heterogeneous signaling dynamics

Receptor tyrosine kinases typically control multiple downstream signaling cascades. It is likely that the combinatorial interplay of these pathways along with differences in signaling dynamics, as found here, defines the specifics of growth factor actions in different cell types. It thus will be important to develop robust live-cell imaging readouts for other signaling modules in order to elucidate the full picture of how growth-factor-mediated signaling dynamics are translated into unique cell behaviors, and how these behaviors influence normal physiology and disease. For instance, we speculate that the brief activation of Akt signaling by EGF is not sufficient to promote cell cycle progression in our model. This would mirror results observed in individual 3T3-L1 cells, in which short-term and low-amplitude stimulation of the PI3K–Akt pathway by PDGF is inadequate to induce translocation of the GLUT4 glucose transporter to the cell membrane (in contrast to the longer and larger effects of insulin; Tengholm and Meyer, 2002). From a more fundamental perspective, comprehensive live-cell imaging studies with multiple readouts should allow for a better understanding of the encoding process, and how downstream pathways are controlled in time and space to trigger distinctive cellular responses (Downward, 2001; Marshall, 1995).

MATERIALS AND METHODS

Reagents

Fetal bovine serum (FBS) was obtained from Hyclone. Dulbecco's modified Eagle's medium (DMEM), FluoroBrite, phosphate-buffered saline (PBS) and trypsin–EDTA solution were purchased from Gibco-Life Technologies. Protease inhibitor tablets were from Roche Applied Sciences, and okadaic acid was from Alexis Biochemicals. Polybrene was purchased from

Sigma-Aldrich, puromycin was from Enzo Life Sciences, 6-well tissue culture dishes were from Greiner Bio-One and 24-well tissue culture plates were from Corning. AquaBlock EIA–WIB solution was from East Coast Biologicals. The following peptide growth factors were purchased from the listed vendors: R3-IGF-I (GroPep), recombinant human PDGF-BB (Invitrogen), mouse EGF (Gibco – Life Technologies), recombinant human PDGF-AA (Thermo Scientific) and recombinant human insulin (Tocris Bioscience). Peptides were solubilized in 10 mM HCl with 1 mg/ml bovine serum albumin, stored in aliquots at −80°C and diluted into FluoroBrite imaging medium immediately before use. Chemical inhibitors included: Linsitinib (ApexBio), Sunitinib (LC Laboratories), PI103 (Tocris Bioscience). All inhibitors were solubilized in DMSO and diluted into imaging medium just before use. A neutralizing antibody to the PDGF-α receptor (#AF1062 final concentration of 2.5 µg/ml) and an isotype-identical negative control antibody (#AB-108-final concentration of 2.5 µg/ml) were purchased from R&D Systems. Other primary antibodies, all purchased from Cell Signaling and used at a dilution of 1:1000, included: anti-phospho-PRAS40 (#2997), anti-PRAS40^{Thr246} (#2691), anti-phospho-Akt^{Thr308} (#2965) and anti-Akt (# 2691). Goat anti-rabbit-IgG conjugated to Alexa-Fluor-680 was from Invitrogen and IR800-conjugated goat anti-rabbit IgG was from Rockland. Other reagents and chemicals were purchased from commercial vendors.

Lentiviral infection and selection

HeLa cells [American Type Culture Collection (ATCC), #CCL2; confirmed to be of human origin and free of contamination] were incubated in Dulbecco's modified Eagle's medium (DMEM) supplemented with 10% FBS. Cells were transduced at 50% of confluent density with concentrated FoxO1–Clover-encoding virus in the presence of polybrene (6 µg/ml), as described previously (Gross and Rotwein, 2013), and sorted using fluorescence intensity with a Becton-Dickinson Influx cell sorter at the OHSU Flow Cytometry Core Facility. Reporter expression was stable for at least ten passages in each sorted cell population. C3H10T1/2 mouse embryonic fibroblasts (ATCC, #CCL226) stably expressing FoxO1–Clover (Gross and Rotwein, 2015), and confirmed to be free of contamination, were maintained under selection with puromycin (2 µg/ml).

Live-cell imaging

Live-cell imaging was performed using an EVOS FL Auto microscope with a stage-top incubator that was maintained at 37°C and 95% humidified air with 5% CO_2. Images were collected at 100× magnification at different intervals using a 10× Fluorite objective (numerical aperture: 0.3) and a GFP light cube (excitation peak, 472/22 nm; emission peak, 510/42 nm). Images were analyzed with the National Institutes of Health ImageJ plug-in Fiji after using the Polynomial Fit plug-in to subtract background fluorescence, the Stack Reg (rigid registration) plug-in to register images and the Gaussian Blur plug-in (at 2 pixels) to average fluorescence across pixels. Individual cells were manually tracked using the mTrackJ plug-in (Meijering et al., 2012) by selecting a single point in the nucleus. Cells that died, divided or migrated out of frame were excluded from analysis. In experiments performed in 6-well dishes, two locations on opposite sides of the well were imaged, whereas for studies using 24-well plates, one central location was imaged. In each location, at least 25 cells were tracked. The relative nuclear intensity of the FoxO1–Clover reporter protein was calculated in each cell by normalizing the values measured at time 0 to 100%. This corresponded to incubation in SFM. In graphs in which single cell responses were plotted with C3H10T1/2 cells, we applied a time-weighted smoothing filter to each data point. This consisted of averaging contributions from the two prior and two succeeding times (adding 50% of the prior or succeeding time point, and 25% of the next succeeding or earlier time point to 100% of the value of the time point in question, and then dividing by 2.5).

Imaging protocols

Short-term responses to individual growth factors

C3H10T1/2 cells were incubated in serum-free Fluorobrite medium plus 2 mM L-glutamine and 0.1% bovine serum albumin for 90 min. Different concentrations of growth factors were added, and images were collected every 2 min for 90 min. Growth factors included insulin (0 to 1400 pM), EGF (0 to 4.2 nM), PDGF-AA (0 to 1400 pM) or PDGF-BB (0 to 104 pM). HeLa cells were incubated in serum-free Fluorobrite medium for 120 min and then incubated with insulin (1400 pM), EGF (4.2 nM), PDGF-AA (3.5 nM), PDGF-BB (4.1 nM) or R3-IGF-I (500 pM), with images collected every 2 min. Sequential growth factor treatments were performed as follows:

C3H10T1/2 cells were incubated in serum-free Fluorobrite medium for 90 min, followed by addition of EGF (4.2 nM) or SFM for 60 min. Either EGF (4.2 nM), R3-IGF-I (500 pM), or SFM was added; images were recorded every 2 min for 120 min.

For antibody-mediated inhibition, C3H10T1/2 cells were incubated in serum-free Fluorobrite medium containing either anti-PDGF-α antibody or IgG (each at 2.5 µg/ml) for 3 h, followed by addition of PDGF-AA (1400 pM) or PDGF-BB (10.4 or 83.2 pM).

For small-molecule-mediated inhibition, C3H10T1/2 cells were incubated in serum-free Fluorobrite medium for 60 min, followed by addition of Sunitinib (0 to 100 nM), Linsitinib (0 to 250 nM) or PI103 (0 to 200 nM) for 30 min. Either PDGF-BB (830 pM) or R3-IGF-I (500 pM) was added, and images were collected every 2 min for 90 min. For all imaging studies, a minimum of three independent experiments were performed.

Protein extraction and immunoblotting

C3H10T1/2 cells that stably expressed FoxO1–Clover were incubated in SFM with Fluorobrite imaging medium for 90 min, followed by addition of insulin (1400 pM), EGF (4.2 nM), PDGF-AA (1400 pM) or PDGF-BB (104 pM). Whole protein lysates were collected after 0, 5, 15, 30, 60 and 90 min of exposure to growth factor by washing cells twice with cold PBS and addition of RIPA buffer containing protease and phosphatase inhibitors (Mukherjee and Rotwein, 2008). Protein aliquots (12.5 µg/lane) were resolved by SDS-PAGE (10% separating gels) and transferred onto Immobilon-FL membranes. Membranes were incubated in 50% AquaBlock for 60 min, followed by addition of primary antibodies at 1:1000 dilution for 16 h, and secondary antibodies for 90 min at 1:5000. Images were collected using the LiCoR Odyssey and analysis software version 3.0 (Lincoln, NE).

Receptor gene expression

The relative amount of each receptor mRNA was assessed using previously published RNA-seq data (ENCODE Project Consortium, 2012). In the UCSC mouse genome browser, the Caltech RNA-seq track for C3H10T1/2 cells was chosen, and for each receptor the peak number of unique reads was determined within a three-exon viewing window.

Acknowledgements

We thank the Oregon Health & Science University Flow Cytometry Core Facility for use of flow-sorting equipment.

Competing interests

The authors declare no competing or financial interests.

Author contributions

S.M.G. and P.R. conceived experiments, S.M.G. performed experiments; S.M.G. and P.R. interpreted results and wrote the manuscript.

Funding

These studies were supported by a National Institutes of Health research grant [grant number R01 DK042748 (to P.R.)]. Deposited in PMC for release after 12 months.

Supplementary information

Supplementary information available online at
http://jcs.biologists.org/lookup/suppl/doi:10.1242/jcs.183764/-/DC1

References

Albeck, J. G., Mills, G. B. and Brugge, J. S. (2013). Frequency-modulated pulses of ERK activity transmit quantitative proliferation signals. *Mol. Cell* **49**, 249-261.

Anastasi, S., Lamberti, D., Alema, S. and Segatto, O. (2016). Regulation of the ErbB network by the MIG6 feedback loop in physiology, tumor suppression and responses to oncogene-targeted therapeutics. *Semin. Cell Dev. Biol.* **50**, 115-124.

Andrae, J., Gallini, R. and Betsholtz, C. (2008). Role of platelet-derived growth factors in physiology and medicine. *Genes Dev.* **22**, 1276-1312.
Batchelor, E., Loewer, A., Mock, C. and Lahav, G. (2011). Stimulus-dependent dynamics of p53 in single cells. *Mol. Syst. Biol.* **7**, 488.
Blakesley, V. A., Scrimgeour, A., Esposito, D. and Le Roith, D. (1996). Signaling via the insulin-like growth factor-I receptor: does it differ from insulin receptor signaling? *Cytokine Growth Factor Rev.* **7**, 153-159.
Borisov, N., Aksamitiene, E., Kiyatkin, A., Legewie, S., Berkhout, J., Maiwald, T., Kaimachnikov, N. P., Timmer, J., Hoek, J. B. and Kholodenko, B. N. (2009). Systems-level interactions between insulin–EGF networks amplify mitogenic signaling. *Mol. Syst. Biol.* **5**, 256.
Brunet, A., Bonni, A., Zigmond, M. J., Lin, M. Z., Juo, P., Hu, L. S., Anderson, M. J., Arden, K. C., Blenis, J. and Greenberg, M. E. (1999). Akt promotes cell survival by phosphorylating and inhibiting a Forkhead transcription factor. *Cell* **96**, 857-868.
Chen, W. W., Schoeberl, B., Jasper, P. J., Niepel, M., Nielsen, U. B., Lauffenburger, D. A. and Sorger, P. K. (2009). Input-output behavior of ErbB signaling pathways as revealed by a mass action model trained against dynamic data. *Mol. Syst. Biol.* **5**, 239.
Cirit, M. and Haugh, J. M. (2012). Data-driven modelling of receptor tyrosine kinase signalling networks quantifies receptor-specific potencies of PI3K- and Ras-dependent ERK activation. *Biochem. J.* **441**, 77-85.
Citri, A. and Yarden, Y. (2006). EGF–ERBB signalling: towards the systems level. *Nat. Rev. Mol. Cell Biol.* **7**, 505-516.
Cross, M. and Dexter, T. M. (1991). Growth factors in development, transformation, and tumorigenesis. *Cell* **64**, 271-280.
Downward, J. (2001). The ins and outs of signalling. *Nature* **411**, 759-762.
ENCODE Project Consortium (2012). An integrated encyclopedia of DNA elements in the human genome. *Nature* **489**, 57-74.
Goh, L. K. and Sorkin, A. (2013). Endocytosis of receptor tyrosine kinases. *Cold Spring Harb. Perspect. Biol.* **5**, a017459.
Gross, S. M. and Rotwein, P. (2013). Live cell imaging reveals marked variability in myoblast proliferation and fate. *Skelet. Muscle* **3**, 10.
Gross, S. M. and Rotwein, P. (2015). Akt signaling dynamics in individual cells. *J. Cell Sci.* **128**, 2509-2519.
Kaushansky, A., Gordus, A., Chang, B., Rush, J. and MacBeath, G. (2008). A quantitative study of the recruitment potential of all intracellular tyrosine residues on EGFR, FGFR1 and IGF1R. *Mol. Biosyst.* **4**, 643-653.
Kubota, H., Noguchi, R., Toyoshima, Y., Ozaki, Y.-i., Uda, S., Watanabe, K., Ogawa, W. and Kuroda, S. (2012). Temporal coding of insulin action through multiplexing of the AKT pathway. *Mol. Cell* **46**, 820-832.
Lam, A. J., St-Pierre, F., Gong, Y., Marshall, J. D., Cranfill, P. J., Baird, M. A., McKeown, M. R., Wiedenmann, J., Davidson, M. W., Schnitzer, M. J. et al. (2012). Improving FRET dynamic range with bright green and red fluorescent proteins. *Nat. Methods* **9**, 1005-1012.
Lehtinen, M. K., Yuan, Z., Boag, P. R., Yang, Y., Villén, J., Becker, E. B. E., DiBacco, S., de la Iglesia, N., Gygi, S., Blackwell, T. K. et al. (2006). A conserved MST-FOXO signaling pathway mediates oxidative-stress responses and extends life span. *Cell* **125**, 987-1001.
Lemmon, M. A. and Schlessinger, J. (2010). Cell signaling by receptor tyrosine kinases. *Cell* **141**, 1117-1134.
Manning, B. D. and Cantley, L. C. (2007). AKT/PKB signaling: navigating downstream. *Cell* **129**, 1261-1274.
Marshall, C. J. (1995). Specificity of receptor tyrosine kinase signaling: transient versus sustained extracellular signal-regulated kinase activation. *Cell* **80**, 179-185.
Meijering, E., Dzyubachyk, O. and Smal, I. (2012). Methods for cell and particle tracking. *Methods Enzymol.* **504**, 183-200.
Mukherjee, A. and Rotwein, P. (2008). Insulin-like growth factor-binding protein-5 inhibits osteoblast differentiation and skeletal growth by blocking insulin-like growth factor actions. *Mol. Endocrinol.* **22**, 1238-1250.
Nelson, D. E., Ihekwaba, A. E., Elliott, M., Johnson, J. R., Gibney, C. A., Foreman, B. E., Nelson, G., See, V., Horton, C. A., Spiller, D. G. et al. (2004). Oscillations in NF-kappaB signaling control the dynamics of gene expression. *Science* **306**, 704-708.
Park, C. S., Schneider, I. C. and Haugh, J. M. (2003). Kinetic analysis of platelet-derived growth factor receptor/phosphoinositide 3-kinase/Akt signaling in fibroblasts. *J. Biol. Chem.* **278**, 37064-37072.
Purvis, J. E., Karhohs, K. W., Mock, C., Batchelor, E., Loewer, A. and Lahav, G. (2012). p53 dynamics control cell fate. *Science* **336**, 1440-1444.
Regot, S., Hughey, J. J., Bajar, B. T., Carrasco, S. and Covert, M. W. (2014). High-sensitivity measurements of multiple kinase activities in live single cells. *Cell* **157**, 1724-1734.
Rena, G., Guo, S., Cichy, S. C., Unterman, T. G. and Cohen, P. (1999). Phosphorylation of the transcription factor forkhead family member FKHR by protein kinase B. *J. Biol. Chem.* **274**, 17179-17183.
Rena, G., Woods, Y. L., Prescott, A. R., Peggie, M., Unterman, T. G., Williams, M. R. and Cohen, P. (2002). Two novel phosphorylation sites on FKHR that are critical for its nuclear exclusion. *EMBO J.* **21**, 2263-2271.
Riese, D. J., Gallo, R. M. and Settleman, J. (2007). Mutational activation of ErbB family receptor tyrosine kinases: insights into mechanisms of signal transduction and tumorigenesis. *Bioessays* **29**, 558-565.
Tang, E. D., Nunez, G., Barr, F. G. and Guan, K.-L. (1999). Negative regulation of the forkhead transcription factor FKHR by Akt. *J. Biol. Chem.* **274**, 16741-16746.
Tay, S., Hughey, J. J., Lee, T. K., Lipniacki, T., Quake, S. R. and Covert, M. W. (2010). Single-cell NF-kappaB dynamics reveal digital activation and analogue information processing. *Nature* **466**, 267-271.
Tengholm, A. and Meyer, T. (2002). A PI3-kinase signaling code for insulin-triggered insertion of glucose transporters into the plasma membrane. *Curr. Biol.* **12**, 1871-1876.
Toettcher, J. E., Weiner, O. D. and Lim, W. A. (2013). Using optogenetics to interrogate the dynamic control of signal transmission by the Ras/Erk module. *Cell* **155**, 1422-1434.
Yissachar, N., Sharar Fischler, T., Cohen, A. A., Reich-Zeliger, S., Russ, D., Shifrut, E., Porat, Z. and Friedman, N. (2013). Dynamic response diversity of NFAT isoforms in individual living cells. *Mol. Cell* **49**, 322-330.
Zhang, X., Gan, L., Pan, H., Guo, S., He, X., Olson, S. T., Mesecar, A., Adam, S. and Unterman, T. G. (2002). Phosphorylation of serine 256 suppresses transactivation by FKHR (FOXO1) by multiple mechanisms. Direct and indirect effects on nuclear/cytoplasmic shuttling and DNA binding. *J. Biol. Chem.* **277**, 45276-45284.

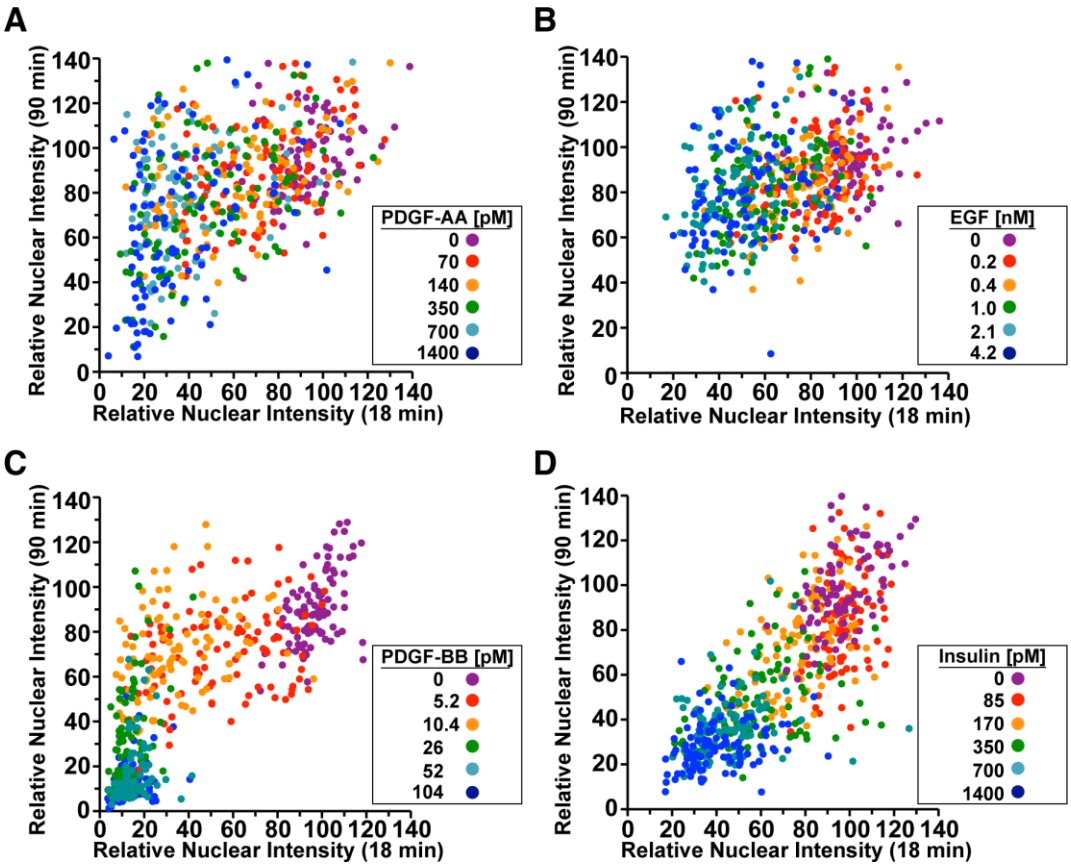

Supplemental Figure 1 (connects to Figures 1-3, 5). Defining growth factor-mediated signaling patterns. Dot-plots illustrating responses of individual cells after incubation with different concentrations of growth factors at 18 and 90 min after their addition (n = 600 cells for each plot, 100 per growth factor concentration). **A**. PDGF-AA; **B**. EGF; **C**. PDGF-BB; **D**. Insulin. For **A** - **D**, growth factor concentrations are indicated by the color-coding.

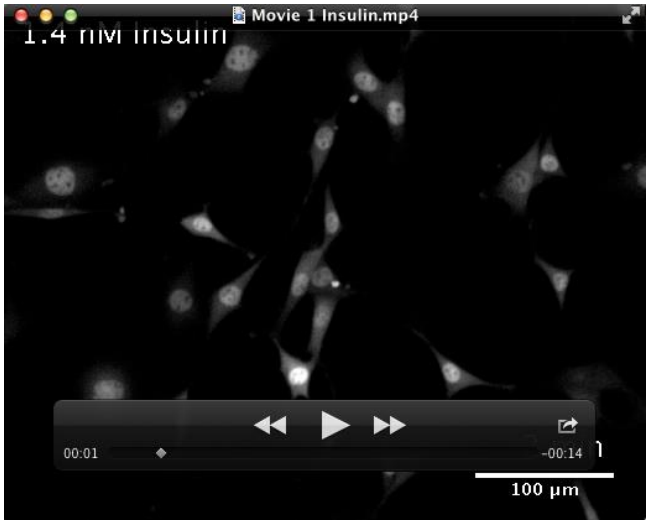

Movie 1 (connects to Figure 1). Subcellular localization of the FoxoO1-clover reporter in C3H10T1/2 cells during exposure to insulin. Cells were incubated in SFM plus insulin [1400 pM], and images were collected every 2 min for 90 min by time-lapse epi-fluorescence microscopy (Evos FL Auto microscope). Images were registered and the background was subtracted as described in Materials and Methods. The video playback rate is 3 frames per second.

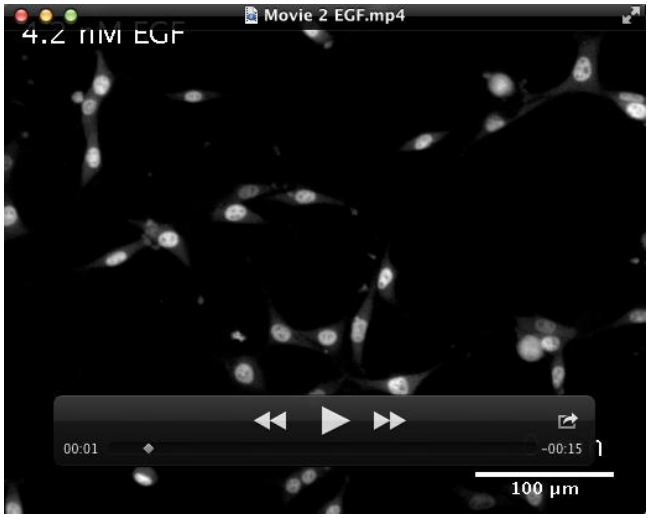

Movie 2 (connects to Figure 2). **Subcellular localization of the FoxoO1-clover reporter in C3H10T1/2 cells during exposure to EGF**. Cells were incubated in SFM plus EGF [4.2 nM], and images were collected every 2 min for 90 min by time-lapse epi-fluorescence microscopy. Images were registered and the background was subtracted as described Materials and Methods. The video playback rate is 3 frames per second.

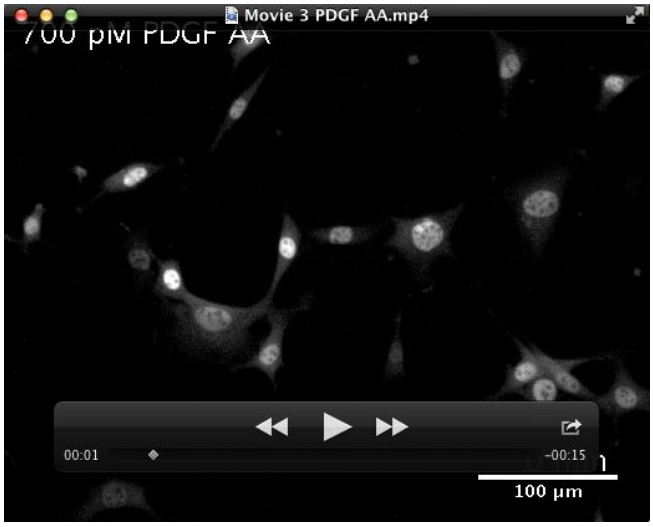

Movie 3 (connects to Figure 4). Subcellular localization of the FoxoO1-clover reporter in C3H10T1/2 cells during exposure to PDGF-AA. Cells were incubated in SFM plus PDGF-AA [700 pM], and images were collected every 2 min for 90 min by time-lapse epi-fluorescence microscopy. Images were registered and the background was subtracted as per Materials and Methods. The video playback rate is 3 frames per second.

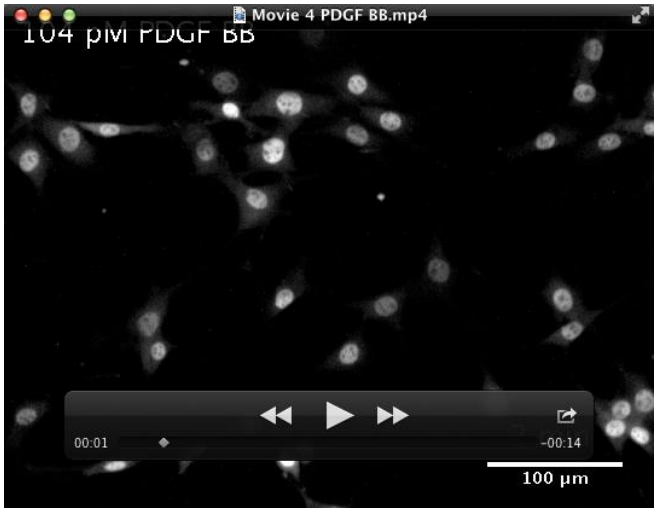

Movie 4 (connects to Figure 5). Subcellular localization of the FoxoO1-clover reporter in C3H10T1/2 cells during exposure to PDGF-BB. Cells were incubated in SFM plus PDGF-BB [104 pM], and images were collected every 2 min for 90 min by time-lapse epi-fluorescence microscopy. Images were registered and the background was subtracted as in Materials and Methods. The video playback rate is 3 frames per second.